ChemComm

COMMUNICATION

View Article Online
View Journal | View Issue

A high-performance alginate hydrogel binder for the Si/C anode of a Li-ion battery†

Cite this: *Chem. Commun.*, 2014, 50, 6386

Received 5th January 2014,
Accepted 18th March 2014

DOI: 10.1039/c4cc00081a

www.rsc.org/chemcomm

Jie Liu,[a] Qian Zhang,[b] Zhan-Yu Wu,[b] Jiao-Hong Wu,[b] Jun-Tao Li,*[b] Ling Huang[a] and Shi-Gang Sun*[ab]

An alginate hydrogel binder is prepared through the cross linking effect of Na alginate with Ca^{2+} ions, which leads to a remarkable improvement in the electrochemical performance of the Si/C anode of a Li-ion battery.

The Li-ion battery (LIB) is one of the most promising energy storage technologies and can enable a wide range of applications, including hybrid electric vehicles and electric vehicles, which are essential in order to reduce fossil fuel dependency. LIBs with high power and high energy are critical for these particular applications. The graphite anodes in current LIBs cannot fulfil these requirements due to their low specific capacity (372 mA h g^{-1}).[1] Silicon (Si) is a promising anode material with a high theoretical specific capacity (4200 mA h g^{-1} for $Li_{4.4}Si$), and a low electrochemical potential of lithiation/delithiation.[2] However, the commercial use of Si-based anodes is still hindered because of two major challenges. One is their low electronic conductivity, leading to poor rate capability, and the other is the huge volume change (400%) during the charge–discharge cycling process, resulting in degradation of the electrode and rapid loss of capacity.[2,3]

To mitigate the volume change effect, many nanostructured Si materials have been designed and synthesized in the last decade, including nanowires,[4–6] nanocrystals,[7] core–shell nanofibers,[8] nanotubes,[9] nanoporous materials[10] and Si–C nanocomposites.[11,12] In order to explore the applications of nanostructured Si materials in LIBs, strong binders are a prerequisite. The binders are critical to maintain the electrode structure and thereby to achieve repeatable LIB operation. Different candidates of new binders for Si-based anodes developed up to now include carboxymethyl cellulose (CMC), poly(acrylic acid) (PAA), polyamide imide (PAI), Na alginate (SA), and so on. Yushin *et al.* demonstrated that the SA binder could yield a stable Si anode in comparison with other polymer binders such as PVDF, PAA, and CMC, resulting in a significant positive impact on the cycle performance of the Si-based electrode.[13] Choi *et al.* developed a mussel-inspired adhesive binder by conjugation of dopamine hydrochloride to the carboxyl groups of SA, which effectively improved the electrochemical performance of the Si anode.[14] In this communication, we report an alginate hydrogel binder through the cross linking effect of SA with Ca^{2+} ions, which remarkably improves the cycleability of a Si/C anode.

Alginic acid, a polysaccharide from seaweed, is a family of natural copolymers of b-D-mannuronic acid (M) and α-L-guluronic acid (G),[15] as illustrated schematically in Scheme 1. In an aqueous solution, the G blocks in different alginate chains undergo ionic cross linking through divalent cations (for example, Ca^{2+} ions), resulting in a network in water, *i.e.* an alginate hydrogel.[15–17] Alginate hydrogel has been studied extensively in the field of tissue engineering as scaffold materials including the regeneration of skin,[18] cartilage,[19] bone,[20] and cardiac tissue.[21] In the present study, alginate hydrogel is applied as a strong binder to improve the electrochemical performance of a Si/C anode. To prepare the alginate hydrogel binder, $CaCl_2$ was dissolved in deionized water to form a solution of 0.26 g L^{-1}. Then SA with a mass of 100 times of $CaCl_2$ was added and then subjected to uniform magnetic stirring.

Fig. 1a presents the XRD patterns of the pure SA binder and the alginate hydrogel binder. The diffractogram of the pure SA binder consists of two crystalline peaks at 2θ = 13.7° and 23.0°.[22,23] After cross linking with Ca^{2+} ions, the intensity of these two peaks is dramatically weakened. This indicates that the SA chains are realigned due to the cross linking effect, resulting in a more amorphous structure. The morphology change between pristine electrodes with pure SA binder and alginate hydrogel binder shown in Fig. S1 (ESI†), visually demonstrating the rearrangement of the SA chains due to the cross linking effect. The FTIR spectrum of pure SA binder in

[a] *State Key Laboratory of Physical Chemistry of Solid Surfaces, College of Chemistry and Chemical Engineering, Xiamen University, Xiamen 361005, China*
[b] *School of Energy Research, Xiamen University, Xiamen 361005, China. E-mail: jtli@xmu.edu.cn, sgsun@xmu.edu.cn; Fax: +86-592-2180181; Tel: +86-592-2180181*

† Electronic supplementary information (ESI) available: Experimental details, TGA curves and XRD patterns of SiNPs, Si–C composite and pure carbon, SEM images of pristine electrodes with pure SA binder and alginate hydrogel binder, cycle performances of Si–C composite electrodes with pure SA binder and alginate hydrogel binder with low ratio of binder (15%), mechanical performance tests. See DOI: 10.1039/c4cc00081a

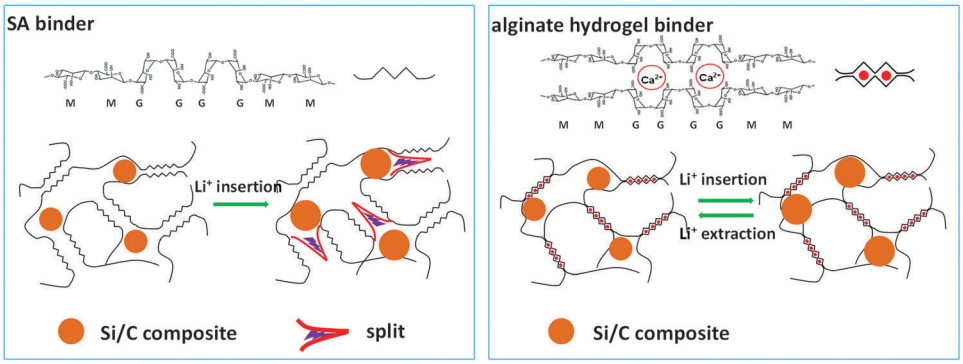

Scheme 1 Effect of the alginate hydrogel binder on the mechanical integrity of the electrode during the cycling processes.

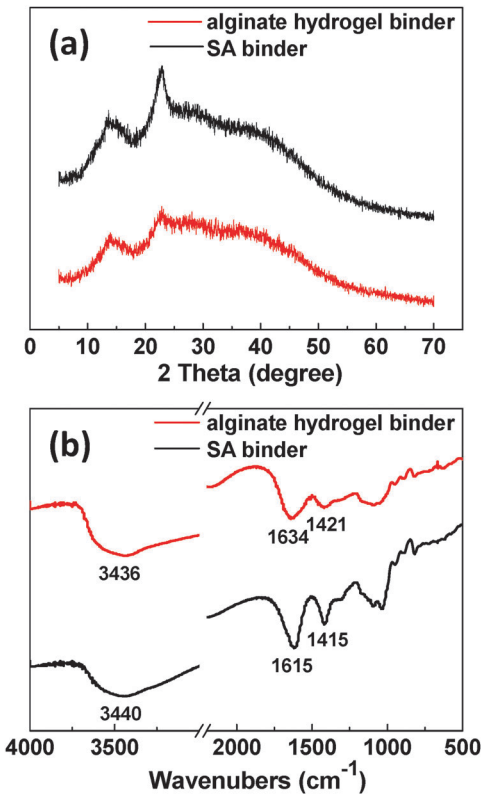

Fig. 1 (a) XRD patterns and (b) FTIR spectra of SA binder and alginate hydrogel binder.

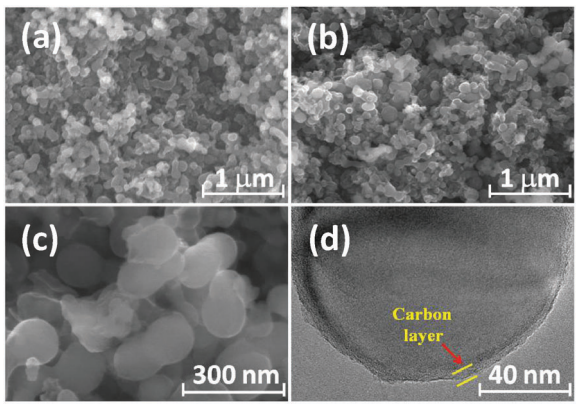

Fig. 2 SEM images of (a) SiNPs, (b) and (c) Si–C composite, and (d) TEM image of Si–C composite.

Fig. 1b shows the bands around 3440, 1615 and 1415 cm^{-1}, ascribed to the stretching of –OH, $–COO^-$ (asymmetric) and $–COO^-$ (symmetric), respectively.[24,25] In comparison with the alginate hydrogel binder, the cross linking process with Ca^{2+} ions causes an obvious shift of the $–COO^-$ stretching bands to higher wavenumbers, indicating the presence of ionic bonding between Ca^{2+} ions and the $–COO^-$ of SA.[24,26]

A Si–C composite was applied as the active material, which was synthesized though pyrolysis of a mixture of Si nanoparticles (SiNPs) and citric acid. The morphology images of the SiNPs and obtained Si–C composite material are presented in Fig. 2. The morphology of the Si–C composite is similar with that of the SiNPs shown in Fig. 2a–c. However, from the TEM image of the Si–C composite, a carbon layer can clearly be seen covering the SiNP (Fig. 2d). TGA (Fig. S2, ESI†) illustrates that the content of Si in the Si–C composite is 80%, and from XRD patterns (Fig. S3, ESI†) only Si phase and carbon phase are observed in the Si–C composite.

Si/C anodes consisting of 53% active material of Si–C composite, 18% carbon black and 29% binder were assembled into 2025 coin cells to evaluate electrochemical performances. Fig. 3a compares the cycle performances of the Si/C anodes with pure SA binder and alginate hydrogel binder at a charge–discharge current density of 420 mA g^{-1} (the first cycles are precycled at 100 mA g^{-1}). The electrode with pure SA binder demonstrates a rapid capacity loss after only 8 cycles, and the discharge capacity decreases to 698 mA h g^{-1} after 120 cycles, *i.e.* a capacity retention of merely 32.5% for the second cycle. However, the cycleability of the electrode with the alginate hydrogel binder is significantly improved. The discharge capacity could maintain a value as high as 1822 mA h g^{-1} after 120 cycles, *i.e.* a capacity retention of 82.3%. Moreover, at a higher charge–discharge current density of 1300 mA g^{-1}, the electrode with the alginate hydrogel binder could also maintain a stable capacity of 1308 mA h g^{-1} after 100 cycles. Even with low ratio of binder (15%) the Si/C electrode with alginate hydrogel binder still exhibits an obviously improved cycle performance (Fig. S4, ESI†).

Fig. 4 compares the charge–discharge curves of Si/C electrodes with pure SA binder and alginate hydrogel binder. As illustrated in Fig. 4a, the discharge potential plateaus of the 50th and 70th

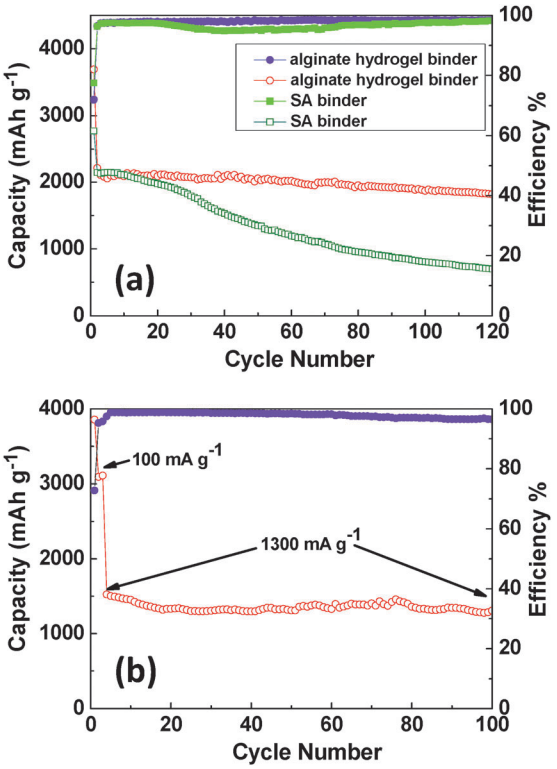

Fig. 3 (a) Cycle performances of Si/C anodes with pure SA binder and alginate hydrogel binder at 420 mA g^{-1}. (b) Cycle performance of Si/C anode with alginate hydrogel binder at a higher current density of 1300 mA g^{-1}.

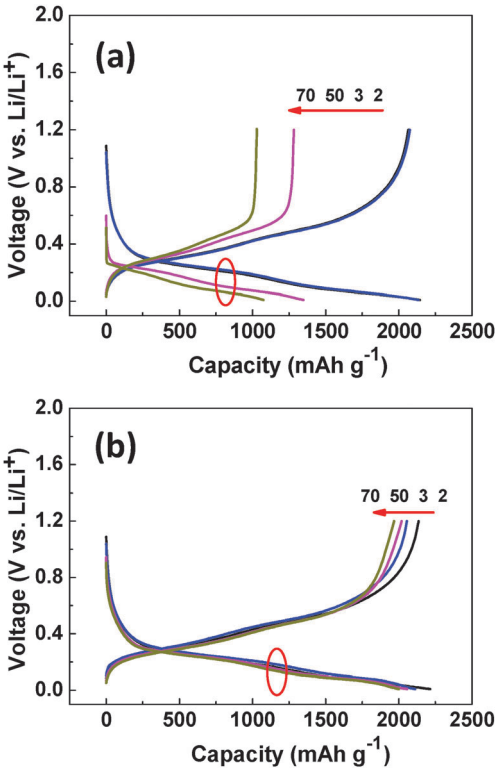

Fig. 4 Charge–discharge curves of Si/C electrodes at 420 mA g^{-1} with (a) pure SA binder and (b) alginate hydrogel binder.

cycles on the electrode with pure SA binder have dropped obviously, indicating that polarization remarkably increases due to the pulverization and fracture of the electrode during charge–discharge cycling processes. However, the potential plateaus of lithiation/delithiation on the electrode with the alginate hydrogel binder are almost unchanged during cycling processes, implying a stable electrode structure.

These improved electrochemical performances are attributed to the network structure formed by cross linking of SA with Ca^{2+} ions, which enhances the mechanical properties of SA,[15–17] demonstrated by the mechanical performance tests shown in Fig. S5–S8 (ESI†). Thereby, it is beneficial to maintain the electrode structure without pulverization and fracture during charge–discharge cycling processes, as illustrated schematically in Scheme 1. When pure SA is used as a binder, the interaction between the SA chains is weak. As a consequence, the electrode would be laniated due to the huge volume expansion of the Si–C composite in the Li^+ insertion process, resulting in the pulverization and fracture of the electrode (Fig. 5a and b) and a poor cycle performance. However, if the alginate hydrogel is applied as a binder, the SA chains firmly cross link together to form a strong-mechanical-property binder. As a consequence, the electrode can maintain an integrated structure without pulverization and fracture (Fig. 5c and d), resulting in a stable cycle performance.

In conclusion, an alginate hydrogel binder has been developed utilizing the cross linking effect between SA and Ca^{2+} ions. This alginate hydrogel binder significantly enhances the mechanical property of SA, and remarkably improves the cycle performance of the Si/C anode of a LIB.

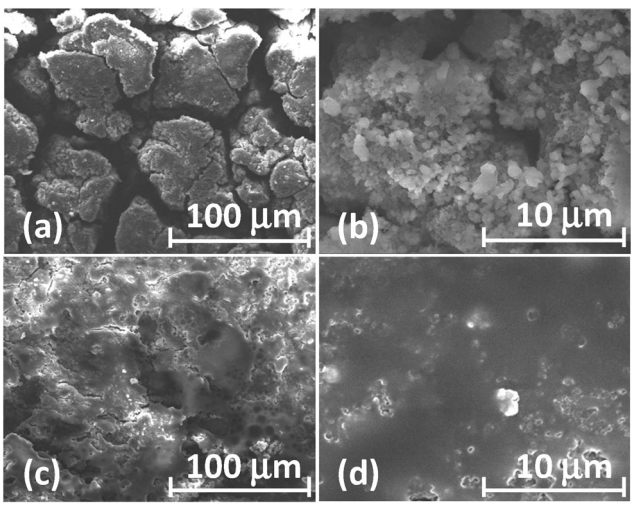

Fig. 5 SEM images of Si/C electrodes after 70 cycles at 420 mA g^{-1} with (a), (b) pure SA binder and (c), (d) alginate hydrogel binder.

This work was financially supported by NSFC (Grant No. 21373008, 21321062), NFFTBS (Grant No. J1310024) and Xiamen Science and Technology Project (3502Z20133002).

Notes and references

1 J. C. Guo and C. S. Wang, *Chem. Commun.*, 2010, **46**, 1428.
2 B. Koo, H. Kim, Y. Cho, K. T. Lee, N. S. Choi and J. Cho, *Angew. Chem., Int. Ed.*, 2012, **51**, 8762.

3 J. S. Kim, W. Choi, K. Y. Cho, D. Byun, J. C. Lim and J. K. Lee, *J. Power Sources*, 2013, **244**, 521.
4 A. S. Arico, P. Bruce, B. Scrosati, J. M. Tarascon and W. V. Schalkwijk, *Nat. Mater.*, 2005, **4**, 366.
5 X. L. Li, J. H. Cho, N. Li, Y. Y. Zhang, D. Williams, S. A. Dayeh and S. T. Picraux, *Adv. Energy Mater.*, 2012, **2**, 87.
6 C. K. Chan, H. L. Peng, G. Liu, K. McIlwrath, X. F. Zhang, R. A. Huggins and Y. Cui, *Nat. Nanotechnol.*, 2008, **3**, 31.
7 H. Kim, M. Seo, M. H. Park and J. Cho, *Angew. Chem., Int. Ed.*, 2010, **49**, 2146.
8 L. F. Cui, R. Ruffo, C. K. Chan, H. L. Peng and Y. Cui, *Nano Lett.*, 2009, **9**, 491.
9 T. Song, J. L. Xia, J. H. Lee, D. H. Lee, M. S. Kwon, J. M. Choi, J. Wu, S. K. Doo, H. Chang, D. S. Zang, H. Kim, Y. G. Huang, K. C. Hwang, J. A. Rogers and U. Paik, *Nano Lett.*, 2010, **10**, 1710.
10 R. Teki, M. K. Datta, R. Krishnan, T. C. Parker, T. M. Lu, P. N. Kumta and N. Koratkar, *Small*, 2009, **5**, 2236.
11 X. Xin, X. F. Zhou, F. Wang, X. Y. Yao, X. X. Xu, Y. M. Zhu and Z. P. Liu, *J. Mater. Chem.*, 2012, **22**, 7724.
12 L. Yue, S. Q. Wang, X. Y. Zhao and L. Z. Zhang, *J. Mater. Chem.*, 2012, **22**, 1094.
13 I. Kovalenko, B. Zdyrko, A. Magasinski, B. Hertzberg, Z. Milicev, R. Burtovyy, I. Luzinov and G. Yushin, *Science*, 2011, **334**, 75.
14 M. H. Ryou, J. Kim, I. Lee, S. Kim, Y. K. Jeong, S. Hong, J. H. Ryu, T. S. Kim, J. K. Park, H. Lee and J. W. Choi, *Adv. Mater.*, 2013, **25**, 1571.
15 C. K. Kuo and P. X. Ma, *Biomaterials*, 2001, **22**, 511.
16 J. Y. Sun, X. H. Zhao, W. R. K. Illeperuma, O. Chaudhuri, K. H. Oh, D. J. Mooney, J. J. Vlassak and Z. G. Suo, *Nature*, 2012, **489**, 133.
17 H. Omidian, J. G. Rocca and K. Park, *Macromol. Biosci.*, 2006, **6**, 703.
18 T. Hashimoto, Y. Suzuki, M. Tanihara, Y. Kakimaru and K. Suzuki, *Biomaterials*, 2004, **25**, 1407.
19 E. Fragonas, M. Valente, M. Pozzi-Mucelli, R. Toffanin, R. Rizzo, F. Silvestri and F. Vittur, *Biomaterials*, 2008, **21**, 795.
20 Y. Ueyama, K. Ishikawa, T. Mano, T. Koyama, H. Nagatsuka, K. Suzuki and K. Ryoke, *Biomaterials*, 2002, **23**, 2027.
21 D. Ayelet, S. Michal, L. Jonathan and C. Smadar, *Biotechnol. Bioeng.*, 2002, **80**, 305.
22 Q. Wang, X. W. Hu, Y. M. Du and J. F. Kennedy, *Carbohydr. Polym.*, 2010, **82**, 842.
23 Q. Wang, Y. M. Du, X. W. Hu, J. H. Yang, L. H. Fan and T. Feng, *J. Appl. Polym. Sci.*, 2006, **101**, 425.
24 S. B. Hua, H. Z. Ma, X. Li, H. X. Yang and A. Q. Wang, *Int. J. Biol. Macromol.*, 2010, **46**, 517.
25 R. Y. M. Huang, R. Pal and G. Y. Moon, *J. Membr. Sci.*, 1999, **160**, 101.
26 Y. M. Xu, C. Y. Zhan, L. H. Fan, L. Wang and H. Zheng, *Int. J. Pharm.*, 2007, **336**, 329.